applied sciences

MDPI

Article

Multiphysics Optimization of a High-Speed Permanent Magnet Motor Based on Subspace and Sequential Strategy

Honglin Yan [1], Guanghui Du [1,*], Wentao Gao [1], Yanhong Chen [1], Cunlong Cui [1] and Kai Xu [2]

[1] School of Electrical and Control Engineering, Xi'an University of Science and Technology, Xi'an 710054, China; yanhonglin2001@163.com (H.Y.); gaowentao0704@163.com (W.G.); chenyanhong@stu.xust.edu.cn (Y.C.); ccunlong@163.com (C.C.)

[2] School of Electrical and Data Engineering, University of Technology Sydney, Sydney, NSW 2007, Australia; kai.xu@student.uts.edu.au

* Correspondence: duguanghui1104@163.com

Abstract: In the optimization of high-speed permanent magnet motors (HSPMMs), electromagnetic characteristics, rotor stress, rotor dynamics, and temperature characteristics must all be considered simultaneously, and there are numerous optimization parameters for both the stator and rotor. These factors pose significant challenges to the multiphysics optimization of HSPMMs. Therefore, this paper presents a multiphysics optimization process for the HSPMM of 60 kW 30,000 rpm by combining subspace strategy and sequential strategy to mitigate the issues of high training volume and mutual coupling. Ten optimization parameters of stator and rotor are determined firstly. Then, using finite element analysis of rotor stress and rotor dynamics, the range of values for critical parameters of the rotor is established. Next, in the electromagnetic optimization, the process is divided into rotor parameter subspace and stator parameter subspace according to the subspace optimization strategy. The temperature field is also checked based on the optimization results. Finally, a prototype is manufactured and the comprehensive performance is tested to validate the multiphysics optimization process.

Keywords: high-speed permanent magnet motor; multiphysics optimization; sequential and subspace optimization strategy

Citation: Yan, H.; Du, G.; Gao, W.; Chen, Y.; Cui, C.; Xu, K. Multiphysics Optimization of a High-Speed Permanent Magnet Motor Based on Subspace and Sequential Strategy. *Appl. Sci.* **2024**, *14*, 8267. https://doi.org/10.3390/app14188267

Academic Editors: Giuseppe Lacidogna and Gerard Ghibaudo

Received: 23 July 2024
Revised: 7 September 2024
Accepted: 11 September 2024
Published: 13 September 2024

1. Introduction

The high-speed permanent magnet motors have the advantages of large power density, small volume, high efficiency, low noise and vibration [1–3]. So, it has broad application prospects in the fields of high-speed motor tools, compressors, blowers, turbine power generation, and has been widely concerned and studied by scientific researchers [4–6]. Due to the high speed and small size of the HSPMM, the design needs to consider the physical field performance such as electromagnetic, loss, mechanical strength, temperature, cooling and heat dissipation, and there are nonlinear and strong coupling relationships between different physical fields [7,8]. Therefore, how to comprehensively analyze and optimize the multiphysics coupling performance of HSPMM has become a challenge task in this field [9–11].

The performance of some HSPMMs has been optimized in existing studies. Some scholars take improving efficiency and torque as optimization objectives, and stator design parameters are set as optimization variables, including air gap, slot size, stator core inner and outer diameter and core length, to optimize a motor with rated power of 6 kW [12]. The effects of sleeve thickness, interference fit, rotor temperature and PM segmentation on rotor stress distribution are investigated in [13,14], which demonstrated that it is reliable to improve the performance of HSPMM by changing key parameters within a small range. For conventional motor, literature [15] presents a multi-objective optimization method based on subspace optimization strategy. The optimization time is shortened effectively by hierarchical optimization of structural parameters through subspace optimization strategy.

In literature [16], a multi-objective optimization method based on sequential optimization strategy is proposed to improve the calculation accuracy of multi-field coupling optimization. The coupling relationship between different physical fields is simplified by artificially specifying the optimal order between different physical fields.

However, studies on optimization of the HSPMM based on subspace and sequential optimization strategies are rare. Specifically, the following problems exist in existing studies:

(1) In current research, scholars focus on the influence of rotor design parameters on motor performance. However, stator design also has a significant impact on the electromagnetic performance, losses, and temperature rise of the motor. Due to the large number of stator parameters, their involvement in optimization can lead to a geometric multiplier increase in optimization training points.
(2) In motor design, the issues within multiple physical fields involve complex interactions and coupling relationships. For example, changes in the electromagnetic field can affect the thermal field distribution, and variations in temperature can, in turn, impact electromagnetic performance. Present optimization studies often consider each physical field independently, overlooking the coupling effects between them. This approach of optimizing a single physical field could yield local optimal solutions rather than global ones.
(3) From the previous literature, the subspace optimization strategy can lower computational problems caused by multiparameter optimization, and the sequential optimization strategy can simplify multi-physics coupling problem. Applying these two optimization strategies to the optimization process of HSPMM may greatly reduce the workload multiplied by multiple optimization objectives. Therefore, it is necessary to explore how to effectively integrate two strategies within the multiphysics optimization of high-speed motors, thereby addressing the optimization challenges posed by multiple parameters and multi-physical fields in high-speed motors. Unfortunately, subspace and sequence optimization strategies are usually used alone in conventional motors, while their combined strategies are missing in the HSPMM.

Therefore, in order to solve the above problems, this paper focuses on multiphysics optimization of the HSPMM by combining the subspace strategy and the sequential strategy. This paper presents a multiphysics optimization design for a 60 kW, 30,000 rpm motor. Initially, a flowchart for the HSPMM multiphysics optimization based on subspace and sequential optimization strategies is designed. According to this flowchart, ten multi-physics optimization parameters are identified. Subsequently, through finite element analysis of rotor stress and rotor dynamics, the range of values for key rotor parameters is determined. Following the subspace optimization strategy, the electromagnetic optimization is divided into rotor parameter subspace and stator parameter subspace, which are then subjected to multi-objective optimization design separately. Through the optimization results, the temperature field of the HSPMM is verified. Finally, based on the optimization results, a prototype of a 60 kW, 30,000 rpm motor is manufactured and tested to validate the analysis presented in this paper.

2. Multiphysics Design Process for HSPMM

Due to the high-speed, high-power density and difficult heat dissipation of HSPMM, rotor stress and rotor dynamics, electromagnetic losses and temperature rise of HSPMM need to be considered [17,18].

In rotor stress and rotor dynamics, sleeve stress of rotor, stress of PM and first-order critical speed of rotor need to be considered. The stress of sleeve and PM of HSPMM should be less than the allowable stress of corresponding material [19]. The first-order critical speed of the rotor structure should be greater with a certain margin than the rated speed, to work below the first-order critical speed.

In the multiphysics optimization of electromagnetic torque and losses, the no-load back electromotive force (EMF), output torque, and PM eddy current loss need to be considered. According to the motor design theory, the no-load back EMF is slightly less than the rated load voltage to ensure that the PM can establish a self-excitation magnetic field so that the motor works in a demagnetization state. With the increase of the speed of HSPMM, in order to keep the motor working in the constant torque region under the condition of constant power, it is necessary to consider the torque above the rated torque. In order to ensure that the motor has high efficiency and the temperature rise of the motor is within the controllable range, in addition to the design of the cooling system, the loss shall be small. The core loss and winding copper loss of the motor are mainly related to the loading power frequency, higher harmonics and material parameters of the motor, so it is necessary to consider the eddy current loss and thermal load of the PM.

According to the general mathematical model of multi-objective optimization problem [20], the optimization mathematical model of the HSPMM can be established as follows:

$$\begin{aligned}
&\text{min}: \quad \begin{cases} f_1\left(\mathbf{x}\right) = \; -T_{\text{average}} \\ f_2(\mathbf{x}) = \; -\eta \\ f_3(\mathbf{x}) = P_{\text{PMloss}} \\ f_4(\mathbf{x}) = AJ \end{cases} \\
&\text{s.t.} \quad \begin{cases} g_1(\mathbf{x}) = F_{\text{sleeve}} - F_{\text{CF}} \leq 0 \\ g_2(\mathbf{x}) = F_{\text{PM}} - F_{\text{NdFeB}} \leq 0 \\ g_3(\mathbf{x}) = n_s - n_{\text{1st}} \times S \leq 0 \\ g_4(\mathbf{x}) = E_0 - U_a \leq 0 \\ g_5(\mathbf{x}) = T_e - T_{\text{average}} \leq 0 \end{cases} \\
&\qquad x_l \leq \mathbf{x} \leq x_u
\end{aligned} \tag{1}$$

where, $T_{average}$, η, P_{PMloss}, represent average output torque, motor efficiency, permanent magnet eddy current loss, respectively and motor thermal load; F_{sleeve} and F_{CF} denote sleeve stress and stress intensity of carbon fiber material, respectively; F_{PM} and F_{NdFeB} represent the stress of PM and the stress intensity of NdFeB material respectively; n_s and n_{1st} represent rated speed of HSPMM and first-order critical speed corresponding to rotor structure respectively, S represents safety factor; E_0 and U_a represent the no-load line back EMF and the loading terminal voltage of the HSPMM respectively; T_e indicates rated torque.

Based on the aforementioned analysis, this study incorporates a multi-physics optimization design methodology for HPMSM, which leverages a subspace and sequential optimization strategy. Firstly, the rotor performance of HPMSM motor is considered, the rotor stress intensity, such as PM stress distribution and sleeve stress distribution, is analyzed, and the value range of rotor main parameters is defined [21]. On this basis, the electromagnetic performance and loss characteristics of the motor for multi-objective optimization design. Finally, through the heat dissipation system design and temperature field verification [22,23], the final multiphysics optimization design scheme is improved. The overall design flow chart is shown in Figure 1.

Step 1: Determine an initial design scheme for that motor according to a conventional motor design theory and a structural size equation of the motor.

Step 2: Analyze rotor stress intensity, including tangential and axial stress distribution of PM and Von-Mises equivalent stress distribution of sleeve.

Step 3: Analyze rotor dynamics modes including first and second-order modes and speeds of the rotor with and without impeller.

Step 4: Determining the value range of the rotor structure parameters based on the analysis results of step 2 and 3 in combination with the allowable stress constraint conditions of the rotor material and the motor structure size equation.

Step 5: Divide optimization design parameters into two subspaces, namely important rotor parameters and important stator parameters, respectively establishing the Kriging proxy model in each subspace and carrying out subspace multi-objective optimization. For the important parameter subspace X1 of the rotor, multi-objective optimization is performed on optimization parameters such as the outer radius of the PM, the thickness of the PM, the thickness of the sleeve and the like based on the value range of the rotor structure parameters in step 4, and three groups of non-inferior optimal solutions are selected to perform multi-objective optimization on the important parameter subspace of the stator. For important stator parameter subspace X2, multi-objective optimization is carried out for optimization parameters such as number of parallel windings, number of conductors per slot and stator slot depth, and three groups of non-inferior optimal solutions are selected for subsequent design.

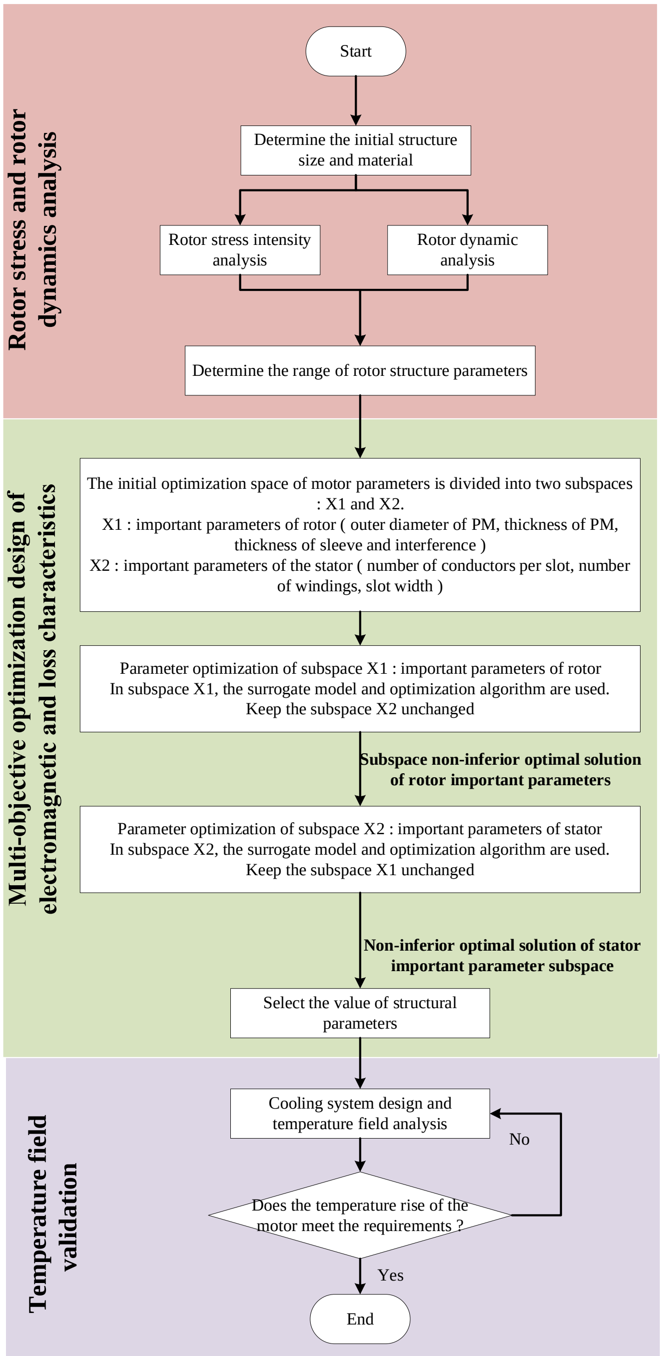

Figure 1. Multiphysics optimization design process.

Step 6: Keep that important parameter subspace X2 of the stator unchanged and carry out multi-objective optimization design on the important parameter subspace X1 of the rotor.

Step 7: Keep that important parameter subspace X1 of the rotor unchanged and carry out multi-objective optimization design on the important parameter subspace X2 of the stator.

Step 8: Select three non-inferior optimal solution sets of electromagnetic performance and loss multi-objective optimization design.

Step 9: Check the temperature field distributions of the three non-inferior optimal solutions according to the cooling system design and select the optimal solution as the final optimal solution.

Step 10: If the temperature fields of the three non-inferior optimal solutions do not meet the engineering requirements, return to redesign the heat dissipation system.

Initially, a two-dimensional finite element model for electromagnetism is developed, which provided the preliminary design parameters for both the stator and rotor. In Ansys Workbench, stress simulations are conducted on the rotor. The rotation speed and interference are added, resulting in a rotor stress response surface. Three-dimensional finite element methods are employed to establish dynamic models of the rotor with and without impellers. The rotation speed and support stiffness are incorporated, and the optimization range for key rotor parameters is determined. Subsequently, a parameterized model is developed with a voltage source established as the excitation condition. Additionally, loss coefficients or conductivity values for materials such as the stator core and permanent magnets are included to discern the loss characteristics of each component. Building on this foundation, before proceeding with electromagnetic optimization, a sensitivity analysis of the optimization parameters is carried out in Ansys Workbench. Pearson's correlation coefficient is applied to obtain a sensitivity analysis chart, which served as the basis for establishing two subspaces. These subspaces are then analyzed through response surface methodology and optimized using a multi-objective genetic algorithm in Workbench, generating the Pareto front. From the Pareto front, three optimal solutions are selected as the final optimization results, and the most suitable solution is chosen according to practical requirements. According to the final structure parameter values of electromagnetic performance and loss optimization, a simulation analysis is conducted in the 3D temperature field. During this procedure, the losses incurred by each component are incorporated as heat sources, and the volume of cooling water is specified.

3. Initial Design Parameters of HSPMM

In this paper, a 60 kW, 30,000 rpm high speed permanent magnet motor with 4 poles and 24 slots, is taken as the research goal object, the stator adopts pear-shaped slot, and the corresponding parameters are shown in Figure 2. According to the basic design method of HSPMM, the initial parameters of relevant parameters are obtained as shown in Table 1 below.

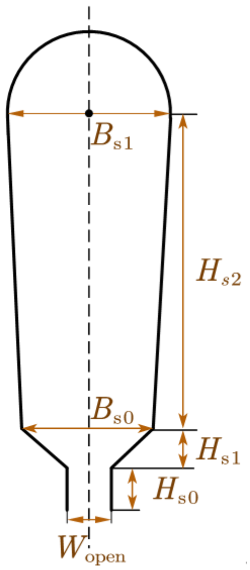

Figure 2. The stator slot shape and its parameters.

Table 1. Initial parameter values.

Name	Initial Design Parameters
Rotor outer diameter (mm)	88.6
Air gap length (mm)	2
Sleeve thickness (mm)	5
PM thickness (mm)	8
Number of conductors per slot	10
H_{s0} (mm)	1
H_{s1} (mm)	0.5
H_{s2} (mm)	16.5
B_{s0} (mm)	3.5
W_{open} (mm)	2

4. Multiphysics Optimization Design

4.1. Rotor Stress and Rotor Dynamics Analysis

Latin hypercube sampling method and Kriging proxy model are used to establish proxy model for rotor stress of HSPMM, as shown in Figure 3. As shown in Figure 3a,b, the radial stress of PM increases gradually with the increase of rotor outer diameter and the decrease of sleeve thickness. In addition, the radial stress of PM presents a saddle curve with the increase of sleeve thickness and interference, which is the same as the variation trend of Figure 3d. Therefore, a certain sleeve thickness and interference can be selected to make the radial stress and tangential stress of permanent magnet obtain non-inferior optimal solutions. As shown in Figure 3c, with the increase of rotor outer diameter and sleeve thickness, there are some non-inferior optimal solution sets for tangential stress of permanent magnet. When rotor outer diameter is 60~100 mm and sleeve thickness is 4~12 mm, tangential stress of permanent magnet obtains non-inferior optimal solution sets. As shown in Figure 3e,f, sleeve stress increases gradually with the increase of rotor outer diameter and sleeve thickness, and sleeve stress increases gradually with the increase of sleeve thickness and interference. Therefore, it is not the case that the greater the thickness of the sleeve, the less the stress on the sleeve will be.

Dynamic rotor models with impeller and without impeller are established by using 3D finite element method. The first-order and second-order critical speeds of rotor under different rotor outer diameters are analyzed, as shown in Figure 4 below. In this analysis, the rotor temperature is set to 110 °C. It can be seen from the figure that the first-order and second-order critical rotational speeds of the rotor gradually increase with the increase of the rotor’s outer diameter. In the stage of smaller rotor outer diameter, that is, when the rotor outer diameter is 40~80 mm, the first-order critical rotational speed of the rotor with impeller increases rapidly. When the rotor outer diameter is 80~100 mm, the first-order and second-order critical rotational speeds of the rotor without impeller gradually exceed those of the rotor with impeller. When the rotor outer diameter is greater than 100 mm, the first-order and second-order critical speeds of the rotor without impeller are higher than those of the rotor with impeller, and the first-order and second-order critical speeds of the two kinds of rotors decrease to some extent. In this paper, the rated speed of HSPMM is 30,000 rpm, rigid rotor is adopted, and the safety factor is 0.75. The first-order critical speed of rotor with impeller should be greater than 40,000 rpm, and the outer diameter of rotor should be in the range of 80~120 mm to meet the requirements of rotor dynamics.

Combined with rotor stress and rotor dynamics analysis, the rotor outer diameter, sleeve thickness and interference can be further restricted. Among them, the value range of the rotor outer diameter is further restricted to 80~100 mm, the sleeve thickness is further restricted to 5~10 mm, and the interference value is 0.05 mm.

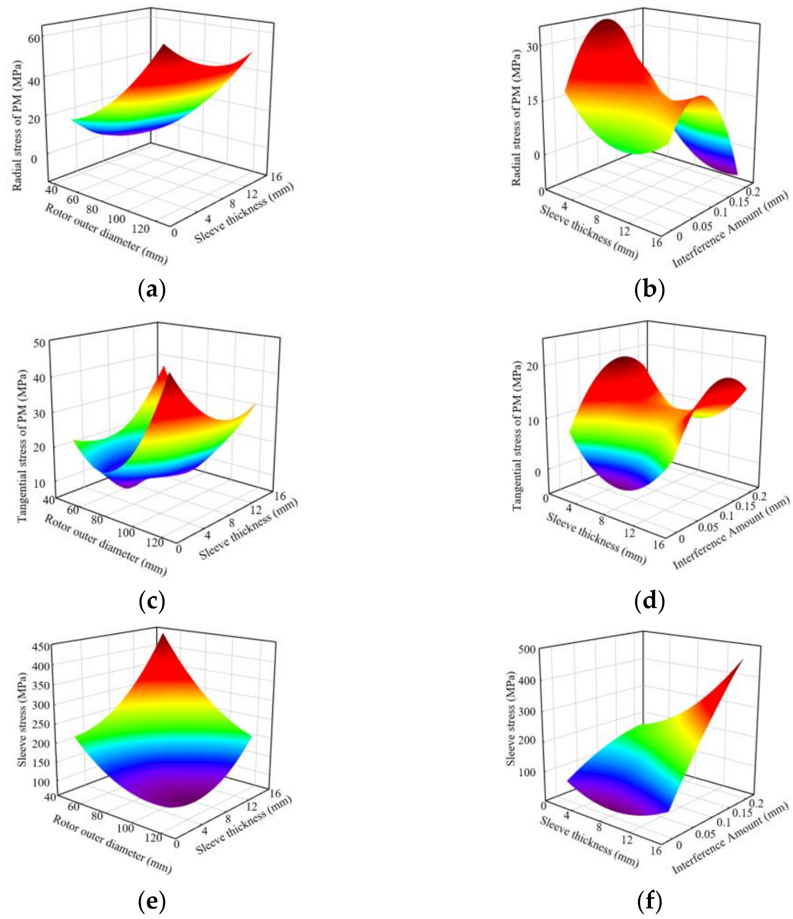

Figure 3. The rotor stress surrogate model of the HSPMM. (**a**) The effect of rotor outer diameter and sleeve thickness on the radial stress of PM. (**b**) The effect of rotor sleeve thickness and interference amount on the radial stress of PM. (**c**) The effect of rotor outer diameter and sleeve thickness on the tangential stress of PM. (**d**) The effect of sleeve thickness and interference amount on the tangential stress of PM. (**e**) The effect of rotor outer diameter and sleeve thickness on the sleeve stress. (**f**) The effect of sleeve thickness and interference amount on the sleeve stress.

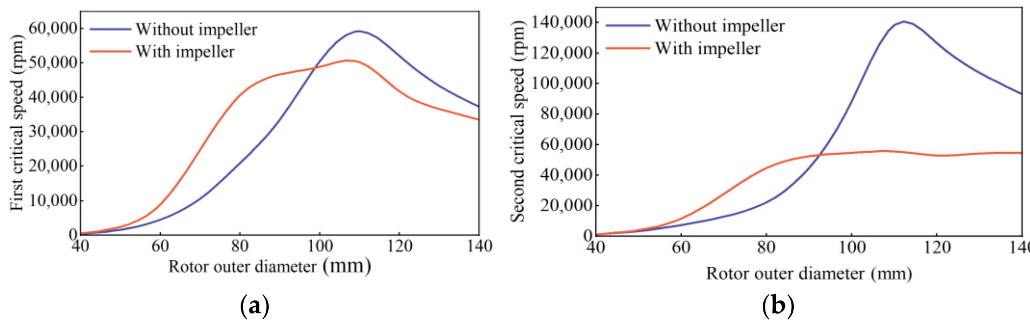

Figure 4. 1st and 2nd critical speeds without impeller and impeller rotor. (**a**) 1st critical speeds without impeller and impeller rotor. (**b**) 2nd critical speeds without impeller and impeller rotor.

4.2. Sensitivity Analysis of Stator and Rotor Parameters

Before electromagnetic performance and loss multi-objective optimization design of HSPMM, sensitivity analysis of main optimization parameters is carried out using a finite element model, and correlation coefficients of each optimization parameter to different optimization objectives are obtained. In this paper, Pearson correlation coefficients are used to express the influence of each optimization parameter on different optimization objectives. The sensitivity of relevant structural parameters is calculated as shown in Figure 5.

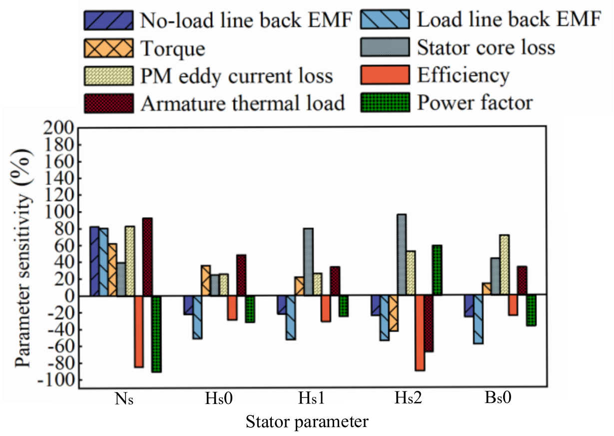

(**a**)

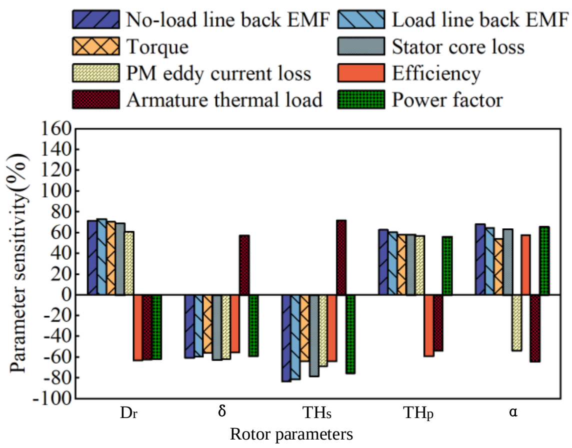

(**b**)

Figure 5. Parameters sensitivity analysis. (**a**) Rotor Parameters sensitivity analysis. (**b**) Stator Parameters sensitivity analysis.

4.3. Multi-Objective Optimization of Electromagnetic Performance and Losses

Establishing a subspace and sequential strategy for high-speed permanent magnet motor multi-objective optimization, the training points for the two optimization strategy is shown in Table 2:

Table 2. Training Points for Multiobjective Optimization.

Name	The Strategy in the Paper Training Points X1		The Strategy in the Paper Training Points X2
Rotor outer diameter	4	256	—
Air gap length	4		—
Sleeve thickness	4		—
PM thickness	4		—
Number of conductors per slot	—		3
H_{s0}	—		3
H_{s1}	—		3
H_{s2}	—		3
B_{s0}	—		3
W_{open}	—		3
All point	256		216

Due to the high sensitivity of subspace X1 to actual parameters, four training points are taken for each parameter within subspace X1, namely the maximum value, minimum value, and two intermediate values, totaling 256 training points. In subspace X2, three training points are selected for each parameter, specifically the maximum value, minimum value, and one intermediate value, summing up to 216 training points. The sensitivity analysis results show that the strategy of optimizing subspace X1 first and then subspace X2 is finally determined.

According to the design requirements, the rated torque of the motor is 19.1 Nm, which is indicated by the light-yellow plane, as shown in Figure 6. As shown in Figure 6a,b, with the increase of sleeve thickness, the output torque first decreases and then increases, while with the increase of permanent magnet thickness, the output torque first increases and then decreases. When the sleeve thickness is greater than 7 mm, the equivalent air gap length of the motor is too large to ensure sufficient excitation magnetic field, so sufficient electromagnetic torque cannot be obtained. As shown in Figure 6c,d, as the outer diameter of the rotor increases and the thickness of the sleeve decreases, the output torque gradually increases. However, as the outer diameter of the rotor increases and the pole arc coefficient increases, the output torque gradually increases. As shown in Figure 6e,f, the output torque of the motor gradually increases as the rotor outer diameter and the air gap length gradually increase, and at the same time, the output torque of the motor also increases as the rotor outer diameter and the permanent magnet thickness gradually increase. However, in the three optimization variables of rotor outer diameter, permanent magnet thickness and air gap length, rotor outer diameter has the most significant influence on motor output torque, which is consistent with the results of parameter sensitivity analysis.

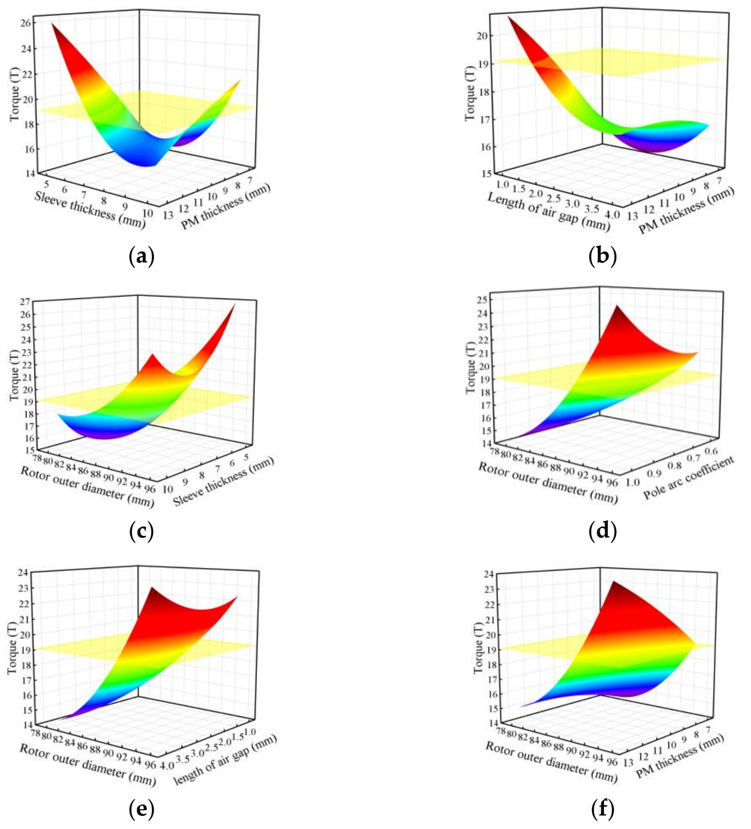

Figure 6. The response surface of output torque. (**a**) The effect of sleeve thickness and PM thickness. (**b**) The effect of length of air gap and PM thickness. (**c**) The effect of rotor outer diameter and sleeve thickness. (**d**) The effect of rotor outer diameter and pole arc coefficient. (**e**) The effect of rotor outer diameter and length of air gap. (**f**) The effect of rotor outer diameter and PM thickness.

The Kriging proxy model of permanent magnet eddy current loss varying with optimization parameters is shown in Figure 7. It can be seen from the figure that the eddy current loss of permanent magnet has several local minima with the change of optimization parameters. The Kriging proxy model established between each optimization parameter and motor efficiency is shown in Figure 8. It can be seen from the figure that almost all the different proxy model surfaces reach the maximum motor efficiency in the middle of the optimization parameter range, and the existing optimization parameters on this surface are reasonable and can meet the optimization conditions of each optimization objective. With the gradual increase of each optimization parameter value, the motor efficiency will gradually reach the local maximum value and then gradually decrease, so there are some local non-inferior optimal solutions of motor efficiency that satisfy the multi-objective optimization mathematical model.

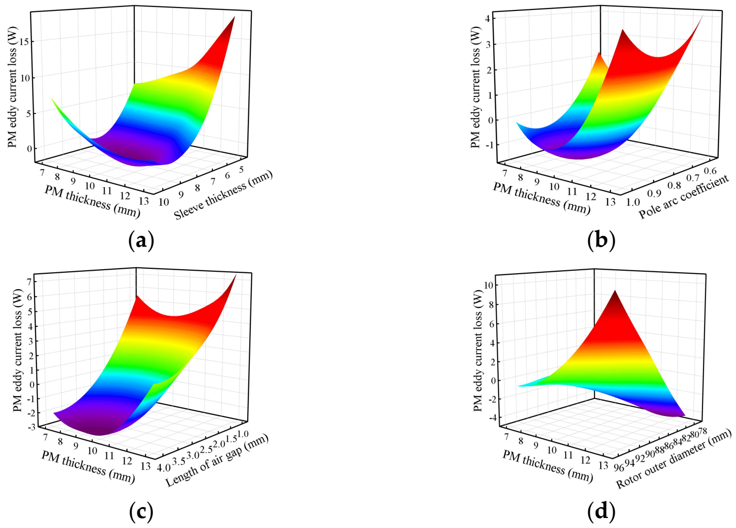

Figure 7. The response surface of permanent magnet loss. (**a**) The effect of PM thickness and sleeve thickness. (**b**) The effect of PM thickness and pole arc coefficient. (**c**) The effect of PM thickness and length of air gap. (**d**) The effect of PM thickness and rotor outer diameter.

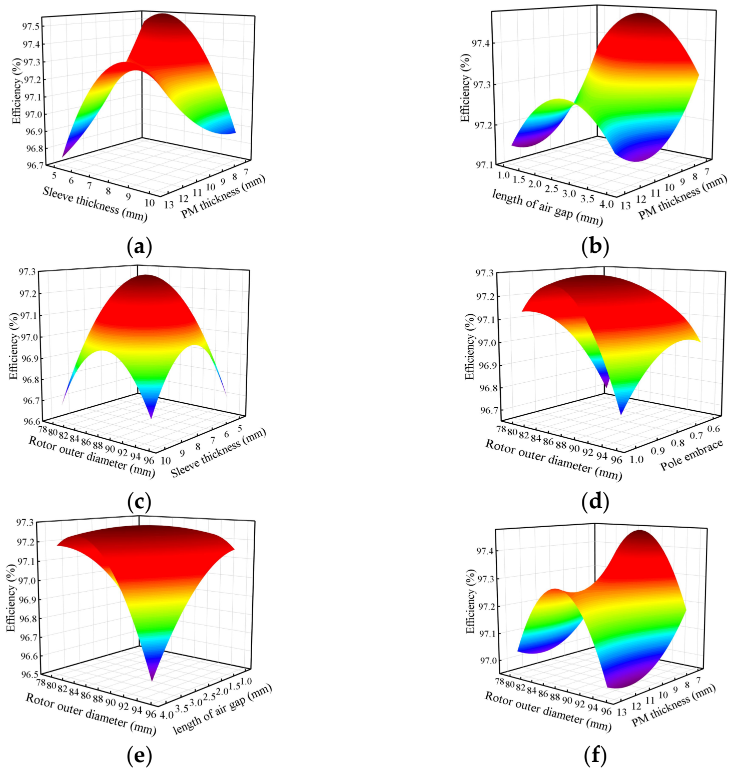

Figure 8. The response surface of efficiency. (**a**) The effect of sleeve thickness and PM thickness. (**b**) The effect of length of air gap and PM thickness. (**c**) The effect of rotor outer diameter and sleeve thickness. (**d**) The effect of rotor outer diameter and pole embrace. (**e**) The effect of length of air gap and rotor outer diameter. (**f**) The effect of length of air gap and PM thickness.

Each optimized parameter has a great influence on the thermal load of the motor winding, as shown in Figure 9 below. According to practical engineering experience and design requirements, the HSPMM designed in this paper only adopts the heat dissipation method of spiral water cooling of the casing, so the thermal load of the motor windings needs to be kept below 250 A^2/mm^3, as shown in the light-yellow plane in the figure below. With the increase of the thickness of permanent magnet, the thermal load of motor windings increases first and then decreases. With the increase of sleeve thickness and air gap length, the thermal load of motor windings increases gradually. In the range of rotor diameter, sleeve thickness, pole-arc coefficient, air-gap length and permanent magnet thickness, Kriging proxy surface model of motor winding thermal load has local optimal solution set, which can be optimized to find non-inferior optimal solution.

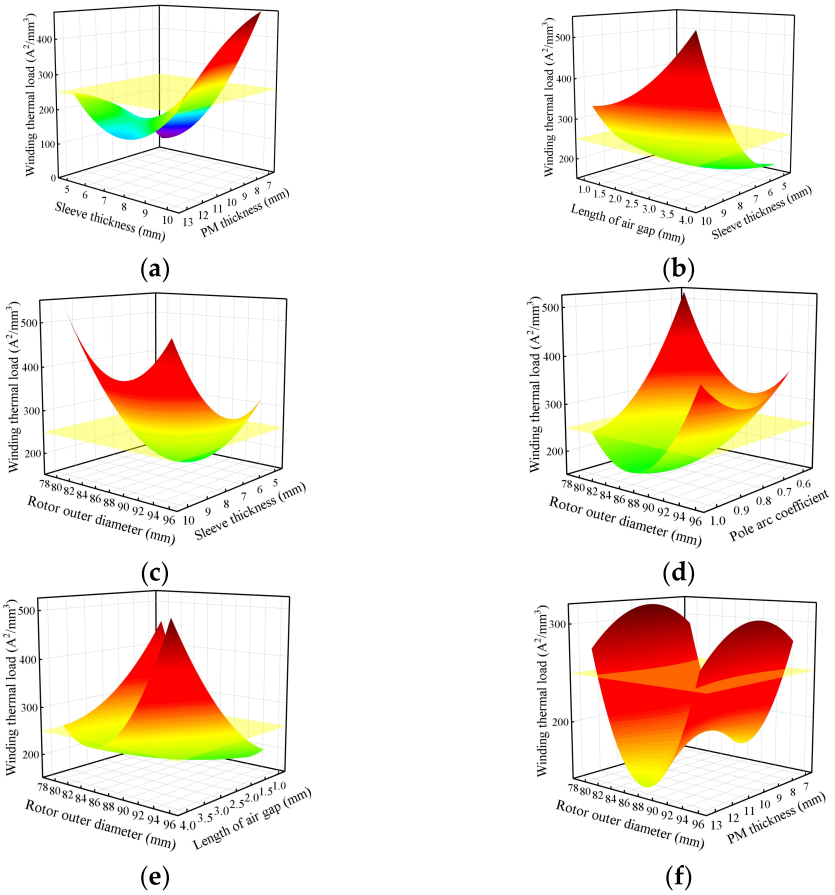

Figure 9. The response surface of thermal load. (**a**) The effect of sleeve thickness and PM thickness. (**b**) The effect of length of air gap and sleeve thickness. (**c**) The effect of rotor outer diameter and sleeve thickness. (**d**) The effect of rotor outer diameter and pole arc coefficient. (**e**) The effect of rotor outer diameter and length of air gap. (**f**) The effect of rotor outer diameter and PM thickness.

Firstly, the Kriging proxy model of the important parameter subspace X1 of rotor is established by keeping the important parameter subspace X2 of stator unchanged, and the Kriging proxy model is optimized by multi-objective genetic algorithm. The resulting Pareto front is shown in Figure 10.

According to the distribution of Pareto front surface, the maximum efficiency of the motor can reach 97.44%, the maximum output torque can reach 20.6 Nm, the minimum eddy current loss of permanent magnet is 4.5 W, and the minimum thermal load of the motor is 122 A^2/mm^3. However, it can be found from Figure 9 that when the motor efficiency is maximum and the motor thermal load is minimum, the permanent magnet eddy current is large and the output torque is small; when the permanent magnet eddy current is minimum and the output torque is maximum, the motor efficiency is small and the motor thermal load is large. Therefore, in multi-objective optimization design, there is not a group of optimal solutions but a compromise choice among all optimization objectives, and the choice space composed of all non-inferior optimal solutions constitutes a Pareto front surface, from which a group of non-inferior optimal solutions satisfying the requirements should be selected as the final optimization scheme.

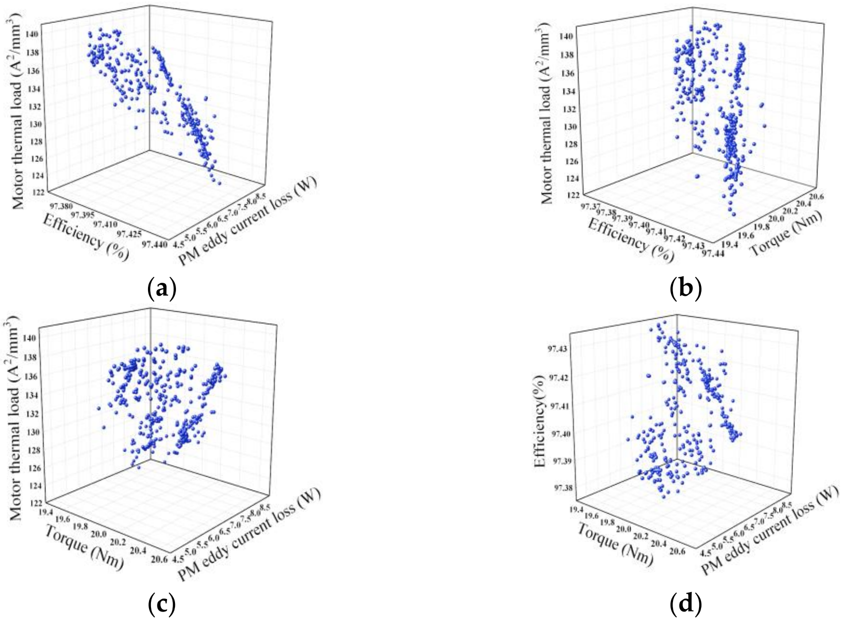

Figure 10. The Pareto solutions of rotor parameters subspace. (**a**) The Pareto solutions of efficiency, PM eddy current loss and motor thermal load. (**b**) The Pareto solutions of efficiency, torque and motor thermal load. (**c**) The Pareto solutions of torque, PM eddy current loss and motor thermal load. (**d**) The Pareto solutions of torque, PM eddy current loss and efficiency.

According to the Pareto front surface of the multi-objective optimization design in the important parameter subspace X1 of the rotor, three non-inferior optimal solutions are selected as candidate values of the final optimization result, as shown in Table 3. The candidate values and the key motor performance parameters corresponding to the initial design are shown in Table 4.

Table 3. Optimal solutions of rotor.

Name	Initial Design	Candidate 1	Candidate 2	Candidate 3
Rotor outer diameter (mm)	88.6	93	93.5	92.5
Air gap length (mm)	2	2.5	2.5	2.5
Sleeve thickness (mm)	5	6	6.5	6.5
PM thickness (mm)	8	12.5	13	12

Table 4. Key performance by the optimized X1.

	Back EMF (V)	Torque (Nm)	PM Loss (W)	Efficiency (%)
Initial design	364	19.1	31.2	96.1
Candidate 1	370	19.6	7.5	97.4
Candidate 2	372	19.7	8.1	97.4
Candidate 3	371	19.6	7.1	97.4

According to the multi-objective optimization results of rotor important parameter subspace, it can be known that the thermal load of the motor is relatively large, although the constraint conditions of Formula (1) are basically satisfied, but it is not ideal. According to the calculation formula and fundamental principle of motor thermal load, it is mainly related to stator important parameters, which is consistent with the results of parameter sensitivity analysis. Therefore, it is necessary to further multi-objective optimization of important parameter subspaces for stators. The main purpose is to further reduce the thermal load of the motor while ensuring that the other optimization objectives are basically unchanged, to reduce the difficulty of heat dissipation of the motor and to ensure that the temperature rise check of the subsequent motor can meet the design requirements.

It can be seen from the three candidate values of rotor important parameter subspace X1 that the performance of the three candidate values is basically the same, while in the optimization of stator important parameter subspace X2, the main objective is to reduce the thermal load of the motor, and the performance of the other optimization objectives can be predicted to have a certain decline. During the rotor parameter design of high speed permanent magnet motor, the thickness of sleeve should be left a certain margin to ensure the safe and stable operation of the motor under special circumstances. Among the three candidate values, candidate value 3 has an ideal sleeve thickness, while meeting the design requirements, leaving a larger margin, and candidate value 3 corresponds to the minimum eddy current loss of the motor performance. Therefore, candidate value 3 is selected as the optimization scheme of the important rotor parameter subspace X1, and input the stator important parameter subspace X2 to carry out subsequent stator important parameter subspace multi-objective optimization.

Under the condition that the value of the optimization candidate solution of the important parameter subspace X1 of the rotor is kept unchanged, the multi-objective genetic algorithm is carried out to optimize the important parameter subspace X2 of the stator, and the thermal load of the motor is further reduced. The resulting Pareto front is shown in Figure 11 below.

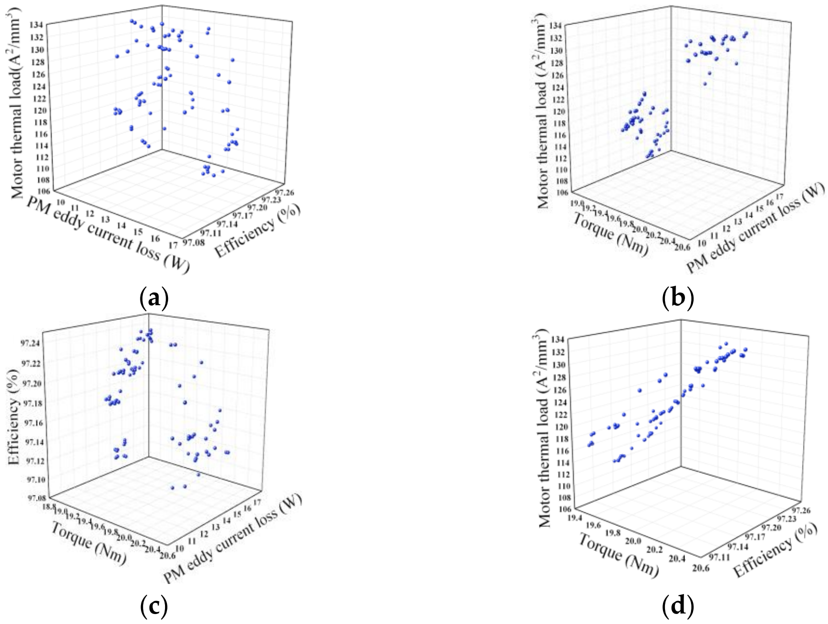

Figure 11. The Pareto solutions of stator parameters subspace. (**a**) The Pareto solutions of PM eddy current loss, efficiency and motor thermal load. (**b**) The Pareto solutions of torque, PM eddy current loss and motor thermal load. (**c**) The Pareto solutions of torque, PM eddy current loss and efficiency. (**d**) The Pareto solutions of torque, efficiency and motor thermal load.

From the Pareto front surface of the important parameter subspace X2, it can be found that the minimum eddy current loss of permanent magnet is 10 W, the maximum output torque is 20.6 Nm, the maximum efficiency of motor is 97.26%, and the minimum thermal load of motor is 106 A^2/mm^3. However, when the eddy current loss of permanent magnet and the thermal load of motor are minimal, the motor efficiency is low and the output torque cannot reach the rated torque requirement. When the output torque is maximum and the motor efficiency is maximum, the eddy current loss of permanent magnet is large and the thermal load of motor is large.

From the Pareto front, the motor efficiency, output torque and permanent magnet eddy current loss after stator important parameter subspace optimization is not as good as those after rotor important subspace optimization. Although these three performances decrease slightly, they fully meet the design requirements of the motor. At the same time, it makes the motor thermal load reduction effect obvious, which is very worthwhile. It can be seen from this that the multi-objective optimization design of motor is a compromise selection of optimization objectives on the Pareto front surface composed of all non-inferior optimal solutions rather than all optimization objectives reaching optimization.

According to the Pareto front surface of the multi-objective optimization design of the important stator parameter subspace X2, the design requirements of the HSPMM are synthesized, and three non-inferior optimal solutions are selected as the candidate values of the final optimization results, as shown in Table 5. The candidate values and the key motor performance parameters corresponding to the initial design are shown in Table 6.

Table 5. Optimal solutions of stator.

Name	Initial Design	Candidate 1	Candidate 2	Candidate 3
Number of conductors per slot	10	8	8	8
H_{s0} (mm)	1	1.5	1.5	1.8
H_{s1} (mm)	0.5	1.2	1.2	1.5
H_{s2} (mm)	16.5	15.5	15.5	15
B_{s0} (mm)	3.5	2	2.2	2.3
W_{open} (mm)	2	2.5	3	2.7

Table 6. Key performance by the optimized X2.

	Back EMF (V)	Torque (Nm)	PM Loss (W)	Efficiency (%)	Thermal Load(A^2/mm^3)
Initial design	364	19.1	31.2	96.1	180
Candidate 1	367	19.1	14	97.18	168
Candidate 2	376	19.3	11	97.27	169
Candidate 3	378	19.7	21	97.09	169

From the three candidate values of stator important parameter optimization subspace X2, it can be seen that the motor performance of the three candidate values greatly reduces the thermal load of the motor under the condition of ensuring that the other optimization objectives are basically unchanged. In order to ensure that the subsequent motor temperature field verification meets the design requirements and the low temperature operation of the high-speed permanent magnet motor, the three candidate values of motor efficiency and winding thermal load are basically consistent, so the minimum eddy current loss of the permanent magnet becomes the priority objective. Therefore, candidate value 2 of the three schemes is selected as the final optimization design scheme of stator important parameter subspace.

After multi-objective genetic optimization of rotor important parameter subspace X1 and stator important parameter subspace X2, and Pareto frontier screening of optimization objectives, the optimized optimization scheme is obtained, as shown in Table 7.

Table 7. The optimization results of electromagnetic performance and loss characteristics.

Name	Initial Parameters	Optimized Parameters
Rotor outer diameter (mm)	88.6	92.5
Air gap length (mm)	2	2.5
Sleeve thickness (mm)	5	6.5
PM thickness (mm)	8	12
Number of conductors per slot	10	8
H_{s0} (mm)	1	1.5
H_{s1} (mm)	0.5	1.2
H_{s2} (mm)	16.5	15.5
B_{s0} (mm)	3.5	2.2
W_{open} (mm)	2	3

4.4. Cooling and Temperature Rise Check

According to the final structure parameter values of electromagnetic performance and loss optimization, the simulation analysis is carried out in the 3D finite element model of temperature field. Since the eddy current loss of permanent magnet and motor efficiency are considered in the optimization process, the temperature field distribution of the optimized motor is different from that of the initial design motor. The temperature field distribution of the two design schemes is shown in Figure 12.

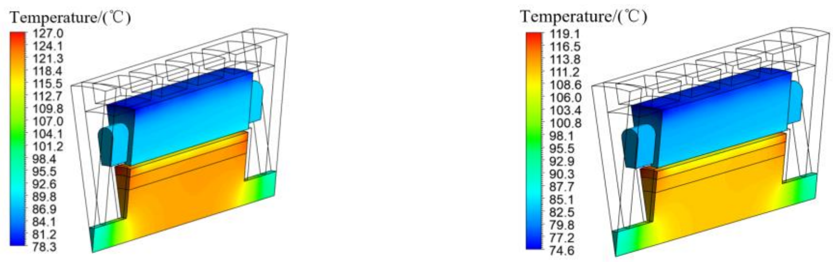

(**a**) (**b**)

Figure 12. Temperature distribution of the HSPMM. (**a**) Initial design. (**b**) Optimized design.

5. Prototype Test Verification

After executing the above multiphysics optimization design for the HSPMM, the final optimization design scheme of the motor can meet the electromagnetic, mechanical and temperature distribution requirements at the same time. In order to better verify the accuracy of the finite element analysis results and the theoretical analysis results, a 60 kW, 30,000 rpm HSPMM is manufactured according to the final optimization design scheme of the HSPMM, as shown in Figure 13.

(**a**) (**b**)

Figure 13. The prototype of the 60 kW 30,000 rpm HSPMM. (**a**) Rotor. (**b**) Prototype.

Rotor stress is the main factor affecting the safe and stable operation of rotor. From the finite element analysis results of the previous optimization design scheme, it can be seen that the radial stress of the permanent magnet is 22 MPa and the sleeve stress is 210 MPa at the rated speed, both of which are far lower than the tensile strength of the corresponding materials. Therefore, the finite element analysis results show that the rotor designed can operate safely and stably at the rated speed. On this basis, the prototype rotor is tested.

After several months of stable operation at rated speed, the rotor is taken out and inspected without any damage. The comparison of the FEA results with the experimental results, as illustrated in Figure 14. It shows that the rotor design is safe and reliable, and there is no resonance phenomenon at rated speed.

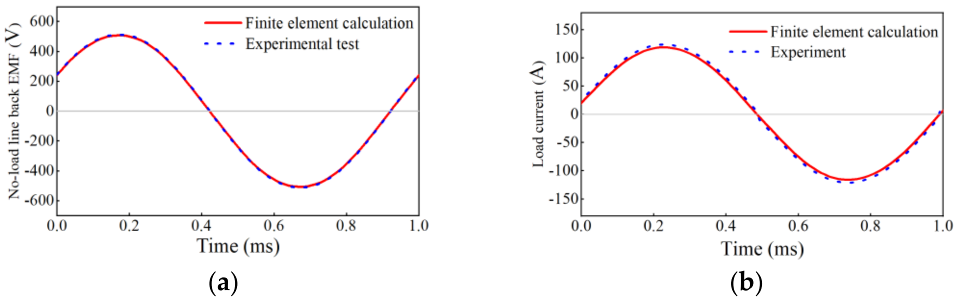

Figure 14. The comparison of the FEA results with the experimental results. (**a**) No-load line back EMF. (**b**) Load current.

The ratio of input power to output power of prototype is 96.9%, which is very close to 97.15% of finite element analysis results. The reason why the actual efficiency is lower than finite element analysis results is mainly due to the actual operating environment temperature and the power loss of rigid connection components such as torque sensor. Install a temperature sensor in the stator winding and measure the temperature of the stator winding under rated operating conditions. During the motor experiment, the water flow rate of the spiral waterway is set to 2 m^3/h, consistent with the finite element calculation. After the prototype runs stably for 2 h, the winding temperature reaches a stable value of 83.3 °C, which is consistent with the temperature field verification analysis result of 87.4 °C.

6. Conclusions

In this paper, an electromagnetic optimization design of a 60 kW, 30,000 rpm HSPMM is carried out. On the one hand, the mechanical strength of the rotor is taken into account in the optimization process. On the other hand, in order to obtain a more reasonable temperature distribution, the maximum motor efficiency and the minimum rotor core loss are selected as the optimization objectives.

This paper introduces a multi-physics field optimization design approach for high-speed permanent magnet motors, streamlining the optimization challenges induced by the coupling of multiple physical fields. Firstly, according to the rotor stress and rotor dynamics finite element analysis results, the value range of the rotor key parameters is determined. Secondly, according to the subspace optimization strategy, the electromagnetic performance and loss multi-objective optimization problem is divided into rotor important parameter subspace and stator important parameter subspace, and multi-objective optimization design is carried out, respectively. On the one hand, the dimensionality reduction optimization of high-dimensional optimization space is realized, on the other hand, the accuracy of Kriging proxy model is guaranteed. Finally, according to the results of electromagnetic performance and loss multi-objective optimization, the temperature field of the designed HSPMM is checked.

After multiphysics optimization design, the efficiency increased by 1.01% and output torque of the motor increased by 1%. the eddy current loss of PM reduces 64.7% and the thermal load of the motor reduces 6.1%. The results of three-dimensional finite element analysis of temperature field show that the overall temperature rise of the motor decreases obviously before and after optimization, and the maximum temperature decreases from 127 °C to 119 °C, decreased by 6.3%. The optimization effect is obvious.

Finally, according to the final optimization results, an experimental prototype is designed and manufactured. The experimental results are basically consistent with the finite element analysis results, which further verify the accuracy of the finite element analysis results and the effectiveness and rationality of the proposed multi-physical field optimization design method for HSPMM.

Author Contributions: Conceptualization, H.Y. and G.D.; methodology, H.Y. and W.G.; software, W.G.; validation, H.Y., G.D., C.C. and K.X.; formal analysis, W.G. and Y.C.; investigation, H.Y. and W.G.; resources, H.Y.; data curation, H.Y., Y.C. and W.G.; writing—original draft preparation, W.G.; writing—review and editing, H.Y., G.D., W.G. and C.C.; visualization, Y.C. and W.G.; supervision, G.D.; project administration, H.Y.; funding acquisition, G.D. All authors have read and agreed to the published version of the manuscript.

Funding: Key Research and Development Program of Shaanxi, 2024GX-YBXM-243. Outstanding Youth Science Fund of Xi'an University of Science and Technology.

Institutional Review Board Statement: Not applicable.

Informed Consent Statement: Not applicable.

Data Availability Statement: The original contributions presented in the study are included in the article, further inquiries can be directed to the corresponding author.

Conflicts of Interest: The authors declare no conflict of interest.

References

1. Nikita, U.; Smirnov, A.; Parks, C.H.; Ahn, J.H.; Heikkinen, J.; Pyrhönen, J. Design aspects of high-speed electrical machines with active magnetic bearings for compressor applications. *IEEE Trans. Ind. Electron.* **2017**, *64*, 8427–8436.
2. Wang, Y.; Feng, J.H.; Guo, S.Y.; Li, Y.F.; Chen, Z.C.; Wang, Y.; Zhu, Z.Q. Investigation of optimal split ratio for high-speed permanent-magnet brushless machines. *IEEE Trans. Magn.* **2018**, *54*, 1–5.
3. Huang, Z.; Fang, J. Multiphysics design and optimization of high-speed permanent-magnet electrical machines for air blower applications. *IEEE Trans. Ind. Electron.* **2016**, *63*, 2766–2774. [CrossRef]
4. Lei, G.; Bramerdorfer, G.; Ma, B.; Guo, Y.; Zhu, J. Robust Design Optimization of Electrical Machines: Multi-Objective Approach. *IEEE Trans. Energy Convers.* **2021**, *36*, 390–401. [CrossRef]
5. Li, Z.; Wang, P.; Liu, L.; Xu, Q.; Che, S.; Zang, L.; Du, S.; Zang, H.; Sun, H. Loss calculation and thermal analysis of ultra-high speed permanent magnet motor. *Heliyon* **2022**, *8*, e11350. [CrossRef] [PubMed]
6. Feng, L.; Liu, W.; Chen, X.; Ding, Y.; Yu, W.; Li, H. Design and optimization of high-speed permanent magnet synchronous motors. *J. Phys. Conf. Ser.* **2024**, *2741*, 012032. [CrossRef]
7. Gieras, J.F. Design of high-speed permanent magnet machines. *Prz. Elektrotechniczny* **2019**, *95*, 1–8. [CrossRef]
8. Li, Y.; Zhu, C.; Wu, L.; Zheng, Y. Multi-objective optimal design of high-speed surface-mounted permanent magnet synchronous motor for magnetically levitated flywheel energy storage system. *IEEE Trans. Magn.* **2019**, *55*, 1–8. [CrossRef]
9. Du, G.; Huang, N.; He, H.; Lei, G.; Zhu, J. Parameter design for a high-speed permanent magnet machine under multiphysics constraints. *IEEE Trans. Energy Convers.* **2020**, *35*, 2025–2035. [CrossRef]
10. Zheng, M.; Huang, W.; Gao, C.; Wu, F. Multiphysics design of a high-speed permanent magnet machine for a micro gas turbine application. *J. Therm. Sci.* **2022**, *31*, 251–260. [CrossRef]
11. Qin, X.; Shen, J. Split ratio optimization of high-speed permanent magnet synchronous motor with multiphysics constraints. *IET Electr. Power Appl.* **2020**, *14*, 2450–2461. [CrossRef]
12. Zhao, X.; Sun, Z.; Xu, Y. Multi-Objective Optimization Design of Permanent Magnet Synchronous Motor Based on Genetic Algorithm. In Proceedings of the 2020 2nd International Conference on Machine Learning, Taiyuan, China, 23–25 October 2020; pp. 405–409.
13. Du, G.; Huang, N.; Zhao, Y.; Lei, G.; Zhu, J. Comprehensive Sensitivity Analysis and Multiphysics Optimization of the Rotor for a High-Speed Permanent Magnet Machine. *IEEE Trans. Energy Convers.* **2020**, *36*, 358–367. [CrossRef]
14. Du, G.; Zhou, Q.; Liu, S.; Huang, N.; Chen, X. Multiphysics Design and Multiobjective Optimization for High-Speed Permanent Magnet Machines. *IEEE Trans. Transp. Electrif.* **2020**, *6*, 1084–1092. [CrossRef]
15. Liu, L.; Li, H.; Dongpo, B. Multi-objective optimization of IPMSM based on subspace division. In Proceedings of the International Conference on Electrical Machines and Systems, Sydney, NSW, Australia, 11–14 August 2017; IEEE: Piscataway, NJ, USA, 2017.
16. Lei, G.; Bramerdorfer, G.; Liu, C.; Guo, Y.; Zhu, J. Robust Design Optimization of Electrical Machines: A Comparative Study and Space Reduction Strategy. *IEEE Trans. Energy Convers.* **2021**, *36*, 300–313. [CrossRef]
17. Du, G.; Huang, N. Multiphysics analysis of high-speed permanent magnet generators for waste heat application. *IET Electr. Power Appl.* **2020**, *14*, 937–942. [CrossRef]
18. Hu, K.; Zhang, G.; Zhang, W. Analysis and optimization of temperature field of high-speed permanent magnet motor. *Adv. Mech. Eng.* **2022**, *14*, 1–11. [CrossRef]
19. Sun, X.; Wan, B.; Lei, G.; Tian, X.; Guo, Y.; Zhu, J. Multiobjective and Multiphysics Design Optimization of a Switched Reluctance Motor for Electric Vehicle Applications. *IEEE Trans. Energy Convers.* **2021**, *36*, 3294–3304. [CrossRef]

20. Barcaro, M.; Bianchi, N. Air-gap flux density distortion and iron losses in anisotropic synchronous motors. *IEEE Trans. Magn.* **2010**, *46*, 121–126. [CrossRef]
21. Xin, C. Comprehensive Design and Multiphysical Analysis of Rotor for High-Speed Permanent-Magnet Motor. Master's Thesis, Shanghai University of Engineering Science, Shanghai, China, 2020.
22. Li, B.; Zhu, J.; Liu, C.; Li, Y.; Lei, G. Comparative study of permanent-magnet synchronous machines with different rotor topologies for high-speed applications. *Appl. Sci.* **2022**, *12*, 4375. [CrossRef]
23. Gu, Y.; Wang, X.; Gao, P.; Li, X. Mechanical analysis with thermal effects for high-speed permanent-magnet synchronous machines. *IEEE Trans. Ind. Appl.* **2021**, *57*, 4646–4656. [CrossRef]